Geomorphology 273 (2016) 335–347

Contents lists available at ScienceDirect

Geomorphology

journal homepage: www.elsevier.com/locate/geomorph

An electric and electromagnetic geophysical approach for subsurface investigation of anthropogenic mounds in an urban environment

Veronica Pazzi [a,*], Deodato Tapete [b], Luca Cappuccini [c], Riccardo Fanti [a]

[a] Department of Earth Sciences, University of Firenze, Via La Pira 4, 50121 Firenze, Italy
[b] British Geological Survey, Natural Environment Research Council, Nicker Hill, Keyworth NG12 5GG, United Kingdom
[c] Department of History, Archaeology, Geography, Fine & Performing Arts (SAGAS), University of Florence, Via San Gallo 10, 50124 Florence, Italy

ARTICLE INFO

Article history:
Received 3 March 2016
Received in revised form 22 July 2016
Accepted 23 July 2016
Available online 26 July 2016

Keywords:
Anthropogenic mound
Urban geomorphology
Archaeological prospection
Geophysical techniques

ABSTRACT

Scientific interest in mounds as geomorphological features that currently represent topographic anomalies in flat urban landscapes mainly lies on the understanding of their origin, either purely natural or anthropogenic. In this second circumstance, another question is whether traces of lost buildings are preserved within the mound subsurface and can be mapped as remnants testifying past settlement. When these landforms have been modified in centuries for civilian use, structural stability is a further element of concern. To address these issues we applied a geophysical approach based on a very low frequency electromagnetic (VLF-EM) technique and two-dimensional electrical resistivity tomography (2D-ERT) and integrated it with well-established surface survey methods within a diagnostic workflow of structural assessment. We demonstrate the practical benefits of this method in the English Cemetery of Florence, Italy, whose mixed nature and history of morphological changes are suggested by archival records. The combination of the two selected geophysical techniques allowed us to overcome the physical obstacles caused by tomb density and to prevent interference from the urban vehicular traffic on the geophysical signals. Eighty-two VLF-EM profiles and five 2D-ERTs were collected to maximise the spatial coverage of the subsurface prospection, while surface indicators of instability (e.g., tomb tilt, location, and direction of ground fractures and wall cracks) were mapped by standard metric survey. High resistive anomalies (>300 and 400 Ωm) observed in VLF-EM tomographies are attributed to remnants of the ancient perimeter wall that are still buried along the southern side of the mound. While no apparent correlation is found between the causes of tomb and ground movements, the crack pattern map supplements the overall structural assessment. The main outcome is that the northern portion of the retaining wall is classed with the highest hazard rate. The impact of this cost-effective approach is to inform the design of maintenance and restoration measures based on improved geognostic knowledge. The geophysical and surface evidence informs decisions on where interventions are to be prioritised and whether costly invasive investigations are needed.

1. Introduction

Urban geomorphology relates to the study of geomorphologic features — of natural, artificial, or mixed origin — in changing and growing urban environments. Geographically confined to areas of concentrated urbanisation (Thornbush, 2015), this discipline also aims to understand how these features reflect the human impact to transform natural terrain into anthropogenic cityscape. In the last 40 years a plethora of studies have investigated the processes and research methods to achieve this knowledge (Coates, 1976; Cooke, 1976; Ahnert, 1998; Bathrellos, 2007; Douglas, 2010; Hudson et al., 2015).

Historically, valleys and alluvial plains were among the preferred landforms to found towns and cities. Nonetheless, natural reliefs and low, rounded hills — the latter commonly referred to as 'mounds' — were exploited owing to their elevation compared with the surrounding flat landscape. These areas were mostly used to install defences, garrisons, or observation points. In other cases, they were considered ideal for civilian uses that needed to be kept separate from the rest of the urban layout, such as cemeteries.

Evidence of the human alteration of local natural features can still be recognised at the ground surface, if the landform is not fully hidden by urban sealing, or caused by those agents that Chengtai (1996) defined as 'artificial geomorphologic'. The public parks of Monte Mario and Colle Oppio in Rome and della Montagnola in Bologna, Italy, are examples of natural mounds and topographic reliefs in old cities that were reshaped and greened during interventions of landscape engineering and architecture in the nineteenth to early twentieth centuries. As a

* Corresponding author.
E-mail addresses: veronica.pazzi@unifi.it (V. Pazzi), deodato@bgs.ac.uk (D. Tapete), luca.cappuccini@unifi.it (L. Cappuccini).

http://dx.doi.org/10.1016/j.geomorph.2016.07.035

consequence, these mounds currently are perceived as green isles within the dense urban fabric and infrastructure built in the mid twentieth to early twenty-first centuries. These situations of mixed artificial and natural ground — compare with 'landscaped ground' definition according to the terminology by McMillan and Powell (1999), Price et al. (2004), and Ford et al. (2010) — can preserve stratigraphic information useful to reconstruct the history of settlement and use or buried remains of lost structures. In this sense urban geomorphology also meets the purposes of archaeological prospection, and this is the framework where this research sits.

The challenge is how to investigate the subsurface without being limited by the physical and environmental constraints and, at the same time, able to gather a sufficient amount of data of suitable resolution to assess the inner structure of the mound. Current morphology, configuration, use, and geographical location of the mound within the urban fabric are among the most common constraints to data accessibility. Furthermore, traditional methods of stratigraphic data collection typically consist of intrusive ground investigations, such as borehole drilling or test-pits and trenches, to expose the subsurface. Apart from being costly, these operations would represent a potential source of damage to the amenity and integrity of the historic assets.

The aim of this paper is therefore to present a geophysical approach based on electric and electromagnetic methods — i.e., very low frequency electromagnetic (VLF-EM) technique and two-dimensional electrical resistivity tomography (2D-ERT) — that can address these issues by exploring the subsurface of anthropogenic mounds in urban environments; relating the observed patterns with historical studies of the geomorphological evolution and surface indicators of ground instability; and finally, providing an evidence base that can inform the decision-making process to plan future ground investigations, maintenance, or repair works.

We implemented our method to the experimental site of the English Cemetery in the city of Florence, Italy. The key questions were: (i) the validation or confutation of the hypothesis that the inner structure of the mound still preserved a section of the perimeter wall formerly connected to the medieval city walls; and (ii) the assessment of the current structural stability of the mound.

As acknowledged by Vitek (2013), technology-led developments can advance field research in geomorphology studies. This paper goes in this direction to demonstrate that a combination of VLF-EM, 2D-ERT, and surface survey can be a viable approach to:

- characterise the structure and composition of the subsurface, thereby proving the archaeological anthropogenic nature of the urban mounds; and
- integrate the stratigraphic findings into the assessment of the structural stability of the mounds.

Notably, the integration of different geophysical methods (e.g., resistivity and VLF-EM: Khalil et al., 2010; Abbas et al., 2012) allows a better data interpretation and improves the level of confidence with regard to the observed patterns. The selection of the geophysical methods is a trade-off between their advantages and intrinsic limitations.

Ground penetrating radar (GPR) has been the most exploited technique in archaeo-geophysics and recently also in the field of nondestructive shallow (<10 m) subsurface forensic investigations (Barone et al., 2016, and literature therein) owing to its properties of high resolution, penetration depth, and fast and cost-effective application (e.g., Griffiths and Barker, 1994; Leckebusch, 2000; Gaffney, 2008; Drahor, 2011; Reynolds, 2011; Goodman and Piro, 2013). Nevertheless, GPR is not suitable for the applications considered in this paper because of: i) the geomorphological conformation of the mound (see Section 2.1); ii) the surface distribution and high density of the monumental tombs that make impossible the use of antennas that have to be coupled with the ground and/or the collection of parallel profiles according to a regular grid (Barone et al., 2016); and iii) the maximum penetration depth of a few meters.

On the other hand, the combination of VLF-EM and 2D-ERT is suitable for implementation in urban contexts where the anthropogenic mounds are surrounded by major city streets with high and constant traffic volumes, and the ground surface is dense with physical obstacles (e.g., poorly distanced tombs in burial ground). Both methods can provide information about the same physical parameter (the soil conductivity or its inverse, i.e., the resistivity); but while VLF-EM is faster, is not affected by physical obstacles, and can provide qualitative areal maps of the measured parameter, 2D-ERT offers higher resolution and provides quantitative information of the electrical properties of the soil. The capability of the VLF-EM to detect buried walls, small-scale conductive and complex structures, was tested by Khalil et al. (2010) and Abbas et al. (2012). In these studies, vertical electrical soundings were integrated with VLF-EM to recognise the general subsurface geoelectric succession and to use the average resistivity value of the media for purposes of a two-dimensional VLF-EM inversion.

This paper is structured as follows: Section 2 provides a description of the English Cemetery, with a complete historical analysis of the geomorphological evolution of the site as inferred from archival documents and paintings; Section 3 details the techniques and methodology; Section 4 presents the results of the geophysical and surface surveys and the data interpretation. The full picture of the subsurface is then discussed in relation to the map of the surveyed surface damages. The latter are used as indicators of the interactions between the artificial ground, exogenous physical agents (e.g., water runoff and infiltration) and current usage of the mound (in the case of the English Cemetery, burial ground with decomposition of organic materials and microcavity generation). Conclusions are drawn to underpin recommendations for strategic planning of preservation measures.

2. Experimental site: English Cemetery, Florence, Italy

2.1. Geomorphologic, geological, and geohazard settings

The English Cemetery of Florence lies on a vegetated mound located in Piazza Donatello (Lat 43.777°; Lon 11.268°) northeast of the town centre (Fig. 1A–B). According to the official cadastre, the oval shape of the cemetery extends NW-SE for >6000 m^2 (~120 m × 64 m; Fig. 1B). The elevation ranges from 51.8 m asl at the southeastern entrance to 58.1 m asl at the top of the northwestern head. Here the drop of ~7 m with regard to the ground level of the road pavement is enhanced by the perimeter retaining walls made of blocks of sandstone (Fig. 1C–D). Therefore, to those coming from the northwest along Viale Giacomo Matteotti, apparently the mound, alongside the neighbouring park of Villa Gherardesca (Fig. 1B), is the most remarkable topographic anomaly of the Florentine urban layout within the enclosure of the nineteenth century boulevards.

According to Tuscany Region (1994), fluvial flooding events are considered 'exceptional' to occur in the whole area. In such circumstances, given the geomorphology and topography of the mound, it is extremely unlikely that the mound itself and the tombs at the top can be flooded, except for the entrance and the southern end which are located at the lowest elevation.

From a point of view of urban geology, no borehole information was available to this study with regard to the Cemetery itself, neither have invasive ground investigations been carried out as part of this research (cf. Section 3), and the authors are not aware of any other previous geological prospection. The closest boreholes are those numbered 1312 and 1636 available from the Municipality WebGIS repository (Comune di Firenze, 2015a) that were drilled in two locations in Borgo Pinti and the park of Villa Gherardesca within a radius of about 200 m from the centre of the mound (Fig. 1B). These boreholes confirm a stratigraphic sequence of alluvial deposits that formed during the depositional

Fig. 1. (A) Aerial view from southeast of the anthropogenic mound in Florence (Italy) above which the English Cemetery was built in the nineteenth century (modified from Google Earth); (B) cadastre plan of the mound and the surrounding historic residential quarters with geographic location in the city map and indication of the boreholes (modified from Comune di Firenze, 2015b); views of (C) the monumental stone façade along the northern section of the retaining wall; and (D) the central pathway connecting the cemetery entrance with the Emperor Frederick William of Prussia's column at the top of the mound (photo credit D. Tapete).

phases of the Florentine alluvial valley. Fig. 2A shows the historical records of piezometric contour lines from early 1970s to 2010, from which it is inferable that no significant alterations were observed underneath the mound in the last decades. No records of groundwater flooding or issues caused by water table rise above normal levels are reported in the published and grey literatures.

Further confirmation that no relevant geohazard factors (e.g., ground motions, land subsidence) affect the mound is gathered through persistent scatterer interferometry (PSI) data. These were accessed via the Extraordinary Plan of Environmental Remote Sensing (METS, 2015) and were analysed using the methodological approach developed by Tapete and Cigna (2012) and Tapete et al. (2015). The PSI data show an overall stability in the last 20 years, from 1992 to 2000 in the ERS-1/2 descending images (Fig. 2B) and from 2003 to 2010 in ENVISAT ascending and descending time series (Fig. 2C). Displacements estimated along the line of sight (LOS) of the satellites take values within the stability threshold (i.e., ± 1.5 mm/y; Fig. 2D). Only in a few cases, persistent scatterers located north of the mound show yearly average LOS velocity of about $+2.2$ mm/y toward the satellite. No patterns of motions are observed, meaning that we can exclude regional-scale land surface or deep geological processes that have impacted the mound by causing instability or structural damages.

2.2. Archaeological setting and conservation history

The importance of preserving the mound also lies in its cultural and historical value. According to the General Regulating Plan (Comune di Firenze, 2015b) an 'extended archaeological bond' applies to the whole quarter and the mound is considered part of the 'historic town centre within the walls'. The mound belongs to 'class 2 - Parks and gardens of particular interest, subzone G2: utilities and services (existing)' and the entrance building is a listed building (class 0) by Italian State Law 1089/39 (Fig. 1B).

Indeed, the morphology of the mound is the result of a long history that can be reconstructed based on a combination of graphic documentation, old maps, and paintings. These documents shed lights on the former condition of the natural relief and the later modifications caused by humans shaping the mound in centuries.

The first known cartographic representation of the mound is included within the copper engraving *Nova pulcherrimae civitatis Florentiae topographia accuratissime delineate* ('New topography of the beautiful city of Florence accurately drawn', Fig. 3A) made by the monk fra Stefano Bonsignori in 1584 and currently belonging to the collection of the Florentine Museum 'Firenze com'era' ('How Florence was'). The mound appears very distinctively beyond the city walls and the gate. Given the detail with which the engraver depicted the urban topography and natural environment, this representation is rather convincing and trustable, although the perspective does not allow us to fully appreciate the planimetric shape of the mound. This, nevertheless, can be derived from a later map of the city of Florence drawn by an unknown geographer in 1690 (Fig. 3B), now accessible at the State Archive of Florence. At this time the mound had a nearly triangular shape, still aligned with the perimeter of the city walls and, particularly, with the barbican that the famous artist Michelangelo Buonarroti designed to protect the city gate. However, in the following decades the wall defences were dismantled and the former triangular shape of the mound was lost and transformed into a more elongate along the walls (Fig. 3C–D). Further changes happened in the second half of the eighteenth century. The city plan by Francesco Magnelli in 1783 shows a circular construction close to the city gate and a short path reaching the top of the relief.

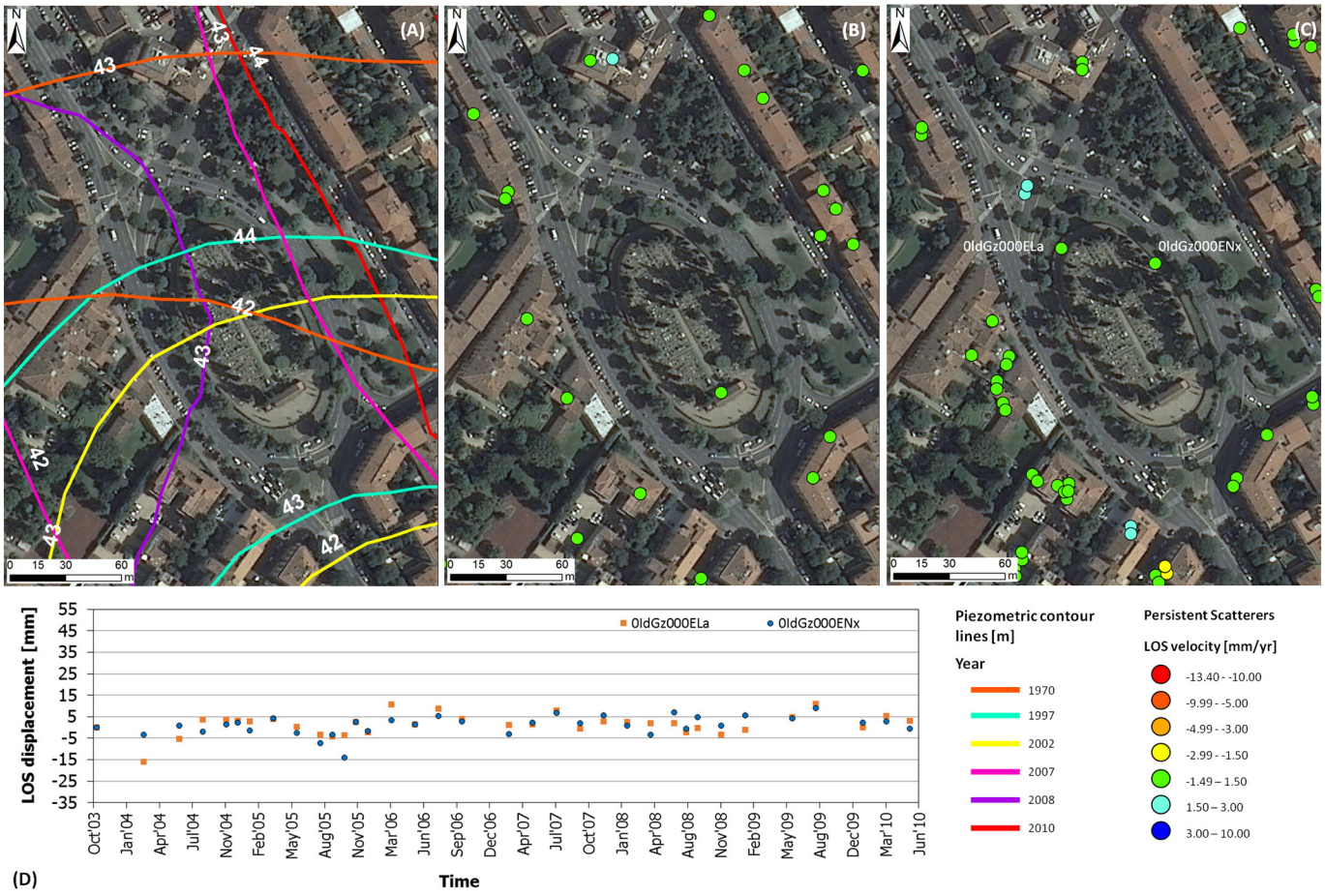

Fig. 2. (A) Isopiezometric contour lines (based on Comune di Firenze, 2015a), (B) ERS-1/2 descending persistent scatterers (PS) 1992–2000, and (C) ENVISAT ascending PS 2003–2010 (METS, 2015) over the English Cemetery and the surrounding residential quarters. (D) Displacement time series of the two ENVISAT ascending PS identified in the northern sector of the mound.

This planimetric representation matches with the coeval engraving *Veduta di Porta a Pinti* ('View of the city gate Porta a Pinti') where we can see some of the key features that currently still characterise the mound (Fig. 3E): trees distributed across the land; the retaining walls made of stones and enclosing the mound along its perimeter; the elevation difference with regard to the ground level. These characteristics are also well documented in the later canvas by Fabio Borbottoni (Fig. 3F). Despite its later date, this painting still documents how the direct connection between the retaining wall and the city walls looked prior to the transformation of the mound into an international and ecumenical cemetery.

In 1827 the Evangelical-Reformed Swiss Church purchased the land and the architect Carlo Reishammer designed the cemetery with all the gravestones and tombs occupying the southern sector of the mound, while the existing circular structure and the vegetation coverage were left in the northern part (Fig. 3G). The latter was instead hugely modified in 1870 by the architect Giuseppe Poggi during his modernisation works of the whole city becoming the capital of the new Italian State. Poggi dismantled the city gate Porta a Pinti, reshaped the English Cemetery into the present oval shape and surrounded the mound with the current boulevards. This made the mound become the green island that it currently is within the cityscape.

Burials were allowed until 1877. Afterward they were banned because the cemetery had become part of the city because of the residential expansion of Florence outside the former walls toward the NE. However, the high density of tombs (1409 in total) had already saturated most of the available space. At present, this is a physical obstacle to account for when planning geophysical prospection (see Fig. 1D).

Wisely, the picturesque character of the cemetery has been preserved throughout the twentieth century, and the current management plan is also ensuring regular maintenance of the trees alongside the restoration of the tombs and gravestones (Fig. 1A,C–D). Notable among the conservation works is the structural intervention needed in 1946 to repair damages caused during WWII bombing of Florence in the northwestern portion of the retaining wall. Recently, the wall was restored again, alongside some graves that were partly collapsed.

In light of the modifications occurring over the past centuries, the recent conservation history is rather important, as it contributed to minimise further alterations of the mound structure. This means that the geophysical prospection presented in this paper relates to a context mostly untouched since the mid nineteenth century.

3. Data and methods

Fig. 4 shows the multistep diagnostic workflow we propose to study anthropogenic mounds by combining the very low frequency electromagnetic method (VLF-EM), bidimensional electrical resistivity tomography (2D-ERT), and surface survey.

This workflow assumes that borehole information might not be available and invasive ground investigation might not have been undertaken before. This is a realistic scenario given that it is quite frequent that conservation needs, urban sealing, architectural obstacles, and cost-effectiveness motivations can represent real-world constraints to access and investigate directly the mound subsurface.

The VLF-EM allows a wealth of data to be collected with limited time consumption over a wide total area of survey, adapting well to

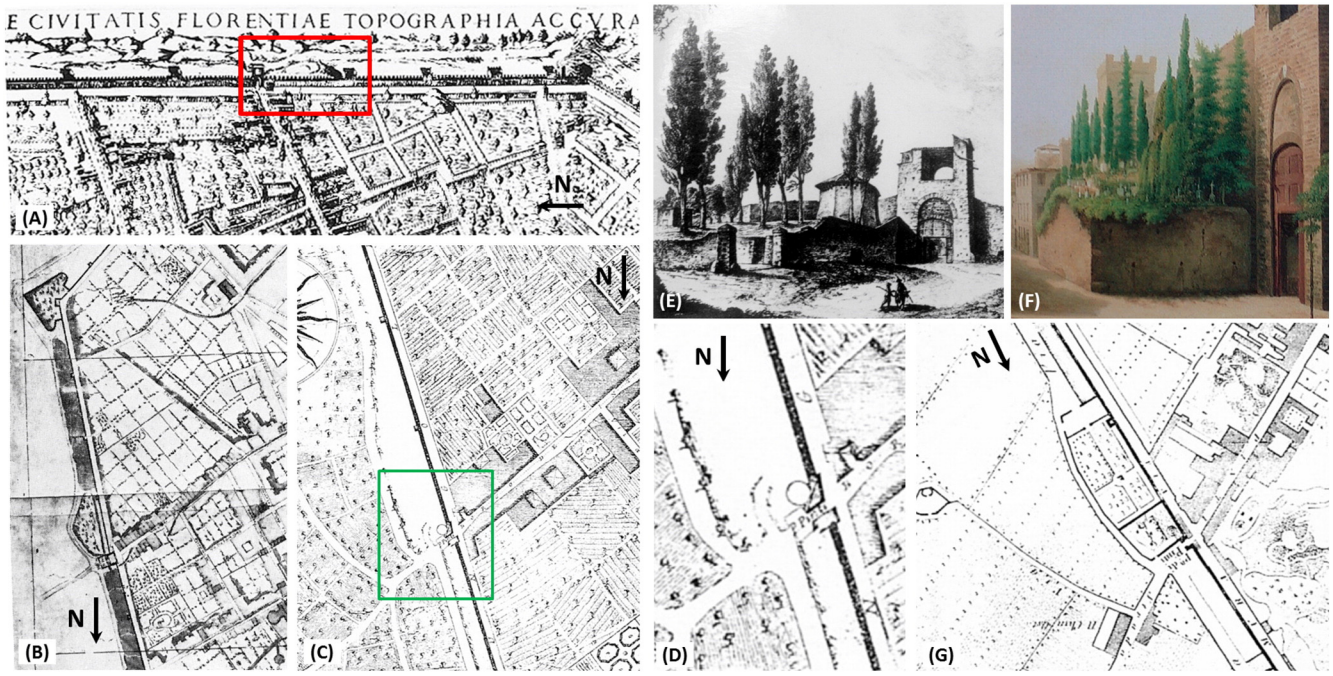

Fig. 3. Natural configuration and human-induced morphological evolution of the mound of the English Cemetery based on historical documentation: (A) fra Stefano Bonsignori (1584) *Nova pulcherrimae civitatis Florentiae topographia accuratissime delineate* with indication of the mound (red square); (B) unknown author (1690) *Pianta della città di Firenze*; (C) Francesco Magnelli (1783) *Pianta della città di Firenze rilevata esattamente nell'anno 1783*; (D) zoom of the circular construction and short path in the northern part of the mound (location in (C), green square); (E) unknown author (second half of the eighteenth century) *Veduta di Porta a Pinti*; (F) Fabio Borbottoni (second half of the nineteenth century) *Porta a Pinti*; (G) Federigo Fantozzi (1843) *Pianta geometrica di Firenze sulla proporzione di 1 a 4500* (all copyrights reserved). (For interpretation of the references to colour in this figure legend, the reader is referred to the web version of this article.)

the morphology and microtopography of the mound surface and overcoming the physical obstacles of local objects such as tombs and gravestones as in the case of the English Cemetery in Florence (see Fig. 5). The spatial distribution of the detected conductive anomalies is then complemented by the quantitative information provided by the 2D-ERT sections that enable a quantitative assessment of the anomaly magnitude and delineation of their boundaries. This workflow therefore optimises the properties of these techniques for implementation in urban contexts, accounting also for the various sources of interference including vehicular traffic noise.

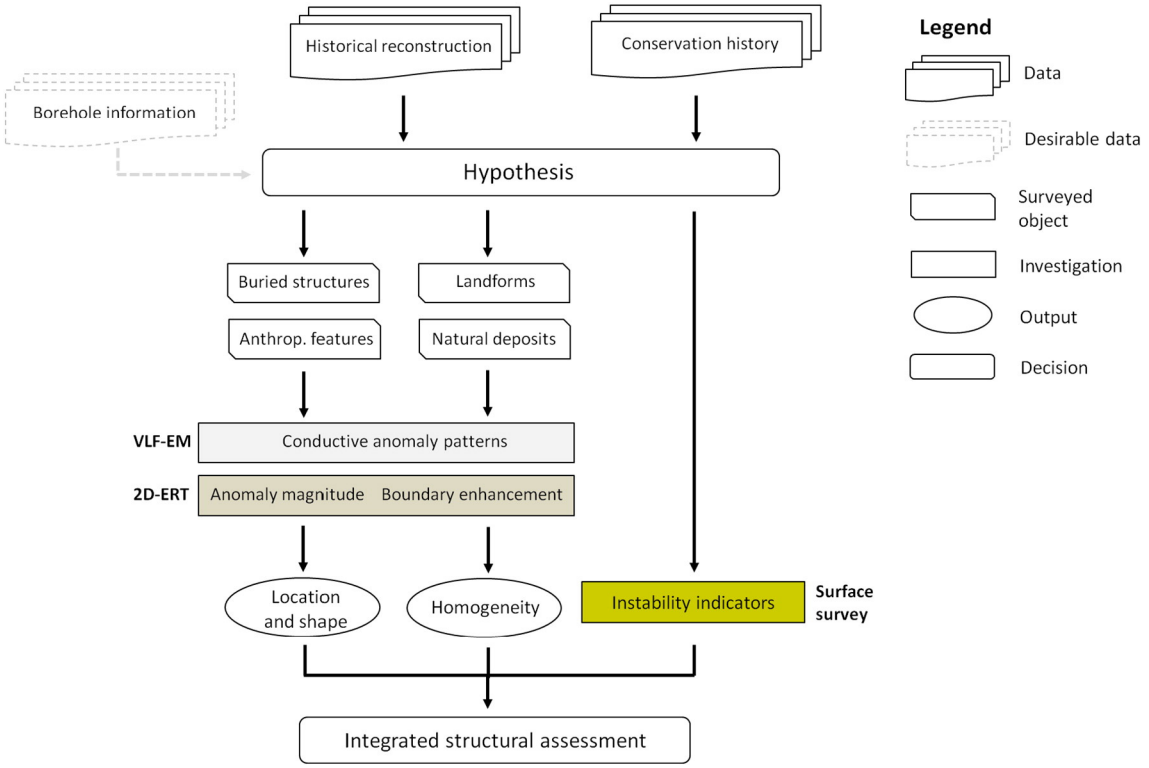

Fig. 4. Flowchart of the electric and electromagnetic geophysical approach proposed and implemented in this research.

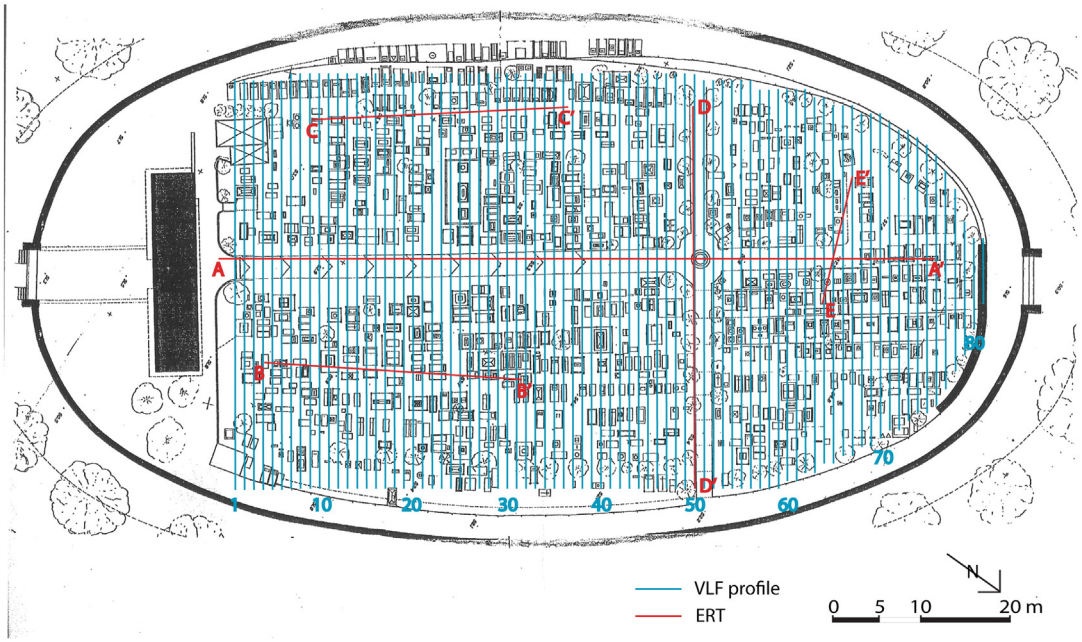

Fig. 5. Plan of the English Cemetery with location of the 82 VLF-EM profiles (blue lines) and the 5 2D-ERTs (red lines). (For interpretation of the references to colour in this figure legend, the reader is referred to the web version of this article.)

3.1. Very low frequency electromagnetic method (VLF-EM)

This method exploits very low frequency signals in the range of 15–30 kHz (Reynolds, 2011). The primary field consists of a horizontal magnetic component Hφ, and an associated vertical electric component E_z, propagating radially outward from the transmitter antenna. Far from the source (i.e., several free wavelengths away) these radio signals can be assumed to be uniform over the survey area, and they can be approximated by H_y. The magnetic component of the primary field, that is perpendicular to the wave propagation direction, induces a secondary horizontal electric component (E_x) in buried conductive structures. This secondary electric current generates a secondary magnetic field that can be measured at the surface by the deviation of the primary VLF field. The resultant elliptically polarized EM field (Smith and Ward, 1974) has two components oscillating in phase and out of phase with the primary field. These components have the same frequency but different amplitude (Khalil et al., 2010; Drahor, 2011; Abbas et al., 2012). The measure of the real and imaginary parts of the vertical secondary magnetic field relative to the horizontal total magnetic field is the essence of the VLF-EM technique. Therefore VLF-EM is based on the ratio between vertical and horizontal components of the local resultant magnetic field that reflect changes in soil resistivity distribution: the vertical component, for example, decreases far from conductors. The VLF-real or in phase component is the amplitude of the component that is in phase with the primary field, while the VLF-imaginary or quadrature component is the out-of-phase component of the secondary field. Both components are expressed as a percentage of the total primary field (Khalil et al., 2010; Bayrak and Şenel, 2012).

In the English Cemetery the VLF-EM survey covered an area of about 4350 m^2, i.e., almost 73% of the total site (Fig. 5). The data were collected with a WADI (ABEM) device and 82 parallel profiles, NE-SW oriented and at equal intervals of 1 m, were measured. The distance between the station points was 1 m apart and the majority of the profiles had a total length of 53 m. A total of 4250 station points were measured during a two-day campaign undertaken by one operator. The transmitter frequency was 22.6 kHz. VLFPROS – Matlab code (Sundararajan et al., 2006) was used for a qualitative interpretation of the VLF-EM data, while filtering procedures according to Fraser (1969) and Karous and Hjelt (1983) were applied to the in-phase component.

The Fraser filter is a band pass filter that calculates the horizontal gradients and smooths the data to give maximum values over conductors (Sundararajan et al., 2006; Khalil et al., 2010; Abbas et al., 2012; Bayrak and Şenel, 2012). The Karous-Hjelt filter, on the other side, generates an apparent current density pseudo-section to determine the current distribution generating the measured magnetic field (Sundararajan et al., 2006). By calculating the inverse filter at different depths, the filter gives an indication about the depth of the various current concentrations (Khalil et al., 2010; Bayrak and Şenel, 2012).

3.2. Bi-dimensional electrical resistivity tomography (2D-ERT)

Direct current (DC) resistivity methods allow calculation of the electrical resistivity of the subsurface. The measurements are made by four electrodes coupled with the soil and applying through two of them (*current electrodes*) a voltage difference (in technical jargon 'current', thus the name of the electrodes) to the soil and measuring the resulting voltage at the other two different electrodes (*voltage electrodes*). Induced current and measured voltage can be correlated, according to the well known Ohm's law:

$$\Delta V = RI \quad (1)$$

where ΔV is the difference of voltage, R is the resistance, and I is the current; and the Pouillet's law:

$$R = \rho\, l/A \quad (2)$$

where R is the resistance of a conductor material with length l, section A, and resistivity ρ.

Through these correlations the apparent resistivity can be retrieved as per the following equation:

$$\rho = k\Delta V/I \quad (3)$$

where k is the geometric factor that depends on the spatial distribution of the four electrodes, i.e., the electrodes array (Koefoed, 1979; Loke

et al., 2013) and the depth of penetration is proportional to the voltage electrodes distance and the electrode array (Dahlin, 2001).

Five 2D-ERTs were collected (Fig. 5) using PASI instrumentation by a team of three people during a one-day campaign. The acquisitions were undertaken using a Wenner-Schlumberger electrode configuration (Loke et al., 2010a; Loke, 2012). Each tomography was handled by means of 32 electrodes, to account for the spatial distribution and density of the tombs and depending on the maximum available horizontal distance achievable (Fig. 6). The main array AA′ was covered by using two chained 2D-ERT with 2-m electrode interval, while the electrode intervals were 1.0 m for the BB′ and CC′ arrays, 1.5 m for the DD′ array, and 0.75 m for the EE′ arrays (Fig. 5). The AA′, BB′, and CC′ arrays were NW-SE oriented and perpendicular to the VLF-EM profiles, while the DD′ and EE′ were NE-SW oriented and parallel to the VLF-EM survey. The apparent resistivity data were inverted by means of the commercial software RES2DINV (Loke and Barker, 1996b; Loke et al., 2010b). The robust inversion was chosen to enhance the sharp boundaries (Loke and Barker, 1996a; Loke et al., 2003), and the model cell size was set at half of the unit electrode spacing (i.e., 1 m for the AA′ array, 0.5 m for the BB′ and CC′ arrays, 0.75 m for the DD′ array and 0.375 m for the EE′ array). The topography correction was applied to all the tomography profiles and the final RMS error of all the profiles was <5%.

3.3. Surface survey

From a morphological point of view, anthropogenic mounds of relatively low elevation and gentle slope angle might be less prone to structural instability and slope failure, unless regional-scale geological processes or human actions such as excavations, infrastructure works, or landscaping interventions impact them directly. Exposure to weathering and processes like water infiltration can favour the triggering of structural instability as a consequence of the mixed natural and artificial character of the mounds.

In this regard the English Cemetery is an interesting exemplar. The historic vegetation coverage is also a potential source of threat because of root-triggered mechanical damages in the near subsurface. In addition, a sealing effect is to be accounted for as a large portion of the total ground surface is currently covered by gravestones that can act as impervious surfaces and allow water to infiltrate via preferential routes only. The latter would not be a serious issue if the runoff was controlled and not constrained by physical obstacles, such as retaining walls, with poorly or discontinuously maintained drainage system.

To collect field evidence of potential structural instability, our geophysical approach also includes a surface survey. This aims to detect and map surface indicators such as damages and cracks caused by the interaction between the above and below-ground components of the mound structure. To this purpose a comprehensive survey was carried out by two operators during a 1-day campaign according to the standards of metric survey (Andrews et al., 2015) to record the tilt of the tombs location and direction of fractures and cracks observed over the mound surface and the stone retaining walls along the whole perimeter of the cemetery and areas of dampness and recent repair. These georeferenced entries were then handled and spatially analysed in a GIS environment to generate a map showing the key areas of concern for conservation.

4. Results and discussion

4.1. Geophysical prospection

The electric and electromagnetic geophysical investigations of the subsurface indicate that the mound is mostly natural. In all five 2D-

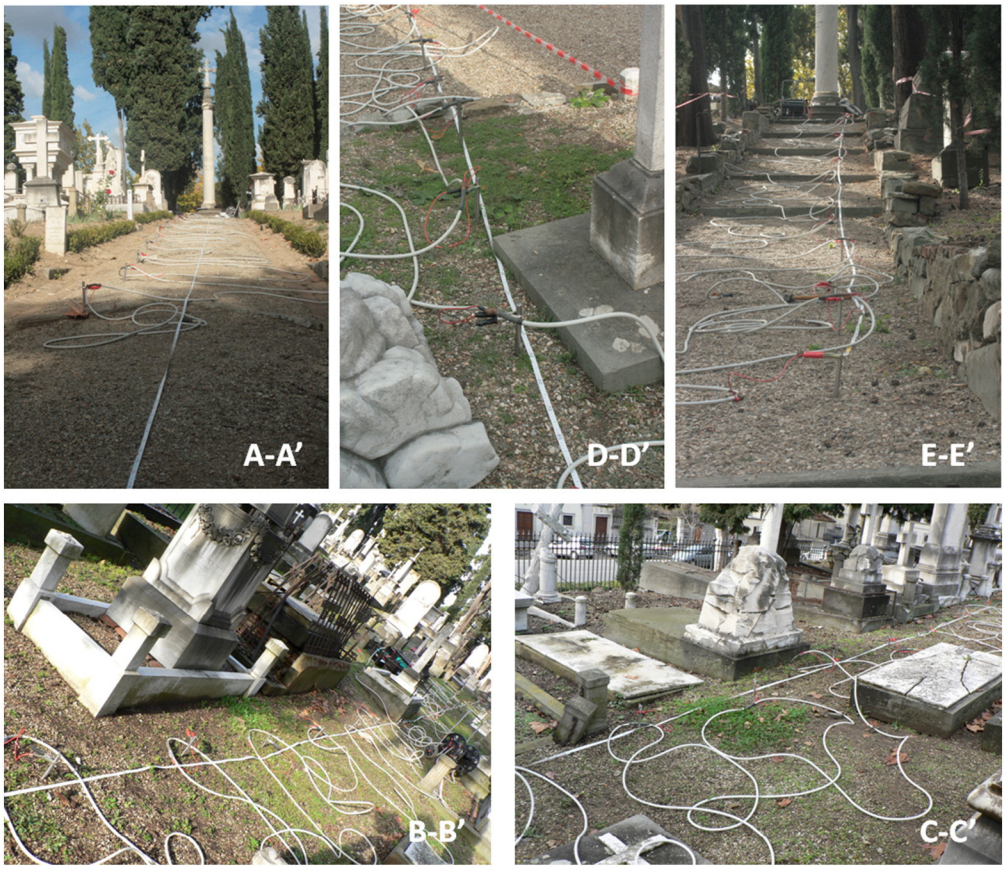

Fig. 6. Flexible arrangement of the 2D-ERT to create suitable cross sections of geophysical prospection across the English Cemetery (from A-A′ to E-E′; for location see Fig. 5), overcoming the physical constraint owing to the high density of tombs and gravestones (photo credit V. Pazzi).

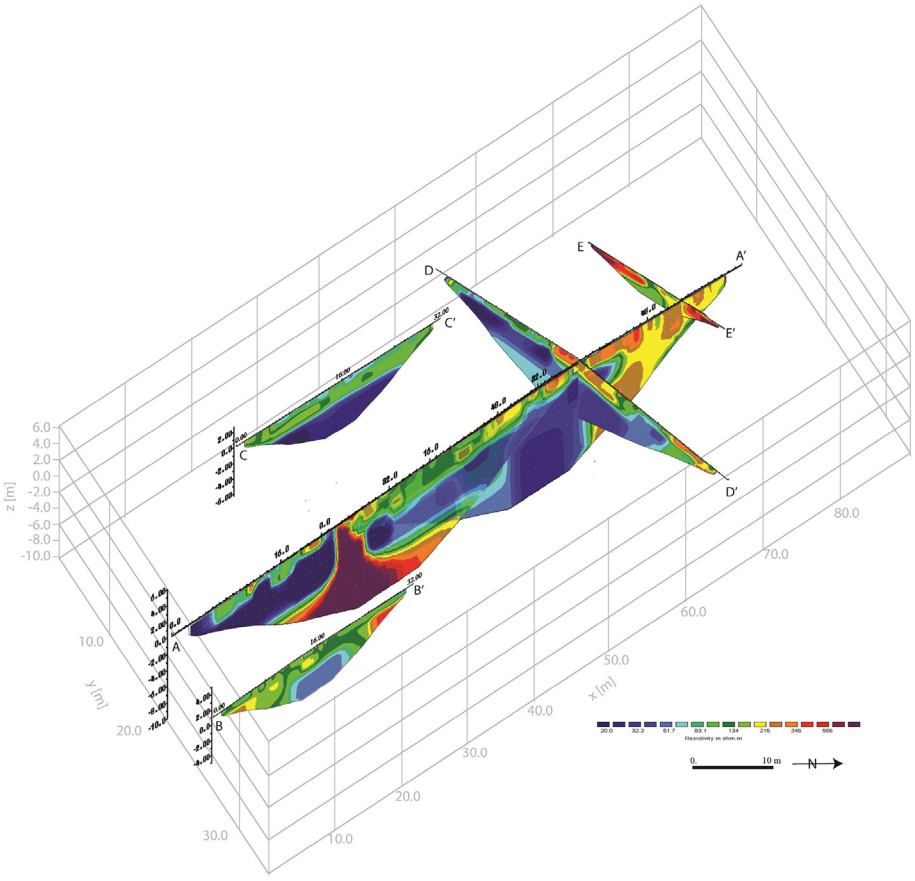

Fig. 7. A 3D view of the five 2D-ERTs (see Fig. 5 for their location and distribution).

ERTs, we can distinguish a conductive bed (<50 Ωm) overlaid up to the surface by a resistive layer (50–150 Ωm) of about 2 m. According to the geology of the area and the two boreholes drilled in the Giardino della Gherardesca (Fig. 1B), lower values of resistivity can be related to silt and saturated loose sands, while higher resistivity to dry sands and gravels. The small resistive anomalies (>200 Ωm) located in the first 2 m can be associated with the tombs. Further non natural elements highlighted by the tomographies are the two high resistive anomalies ((i) >400 Ωm and (ii) >300 Ωm in Fig. 7 and Fig. 10) along the AA′ profile. These are more likely caused by anthropogenic structures than natural structures because of their shapes and resistivity. The shape of the anomaly (i), in fact, reminds us of a section of wall or something similar, while its high resistivity value can be associated with cement. Moreover, the shape and the resistivity could also be associated with a void or a cavity.

The curves displayed in Fig. 8 consistently show peaks of VLF amplitude that identify VLF-EM trends across the collected profiles. This result corroborates the interpretation of the anomalies observed in the 2D-ERTs and suggests that the buried section of the ancient wall extends across the width of the southern portion of the mound.

Given the measured depth, a shallow archaeological test-pit dig out at the middle of the pathway linking the entrance to the votive column in the centre of the cemetery (Fig. 1D) may reveal the remains of the wall or of the cavity a few meters from the ground surface.

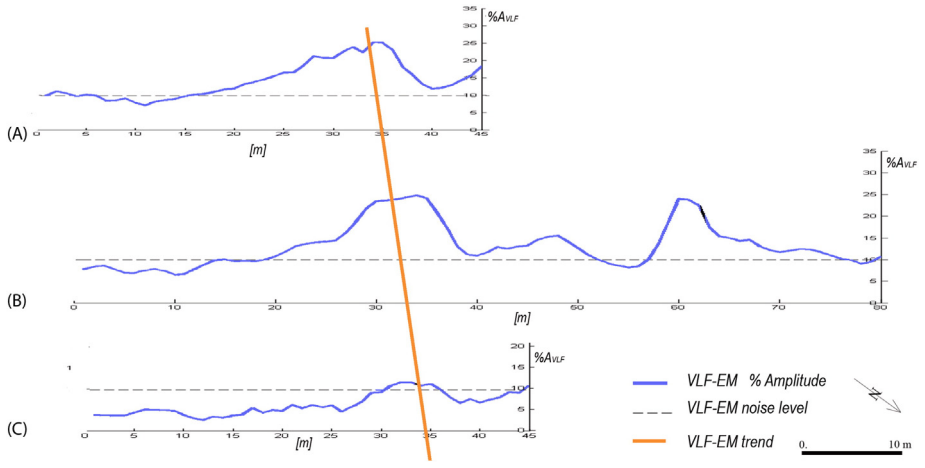

Fig. 8. VLF amplitude (%) obtained by extracting, from the collected profiles, the values corresponding to the 2D-ERT CC′ (A), AA′ (B) and BB′ (C): higher values of the VLF-EM amplitude are associated with the high resistivity anomalies. The orange line highlights this correlation.

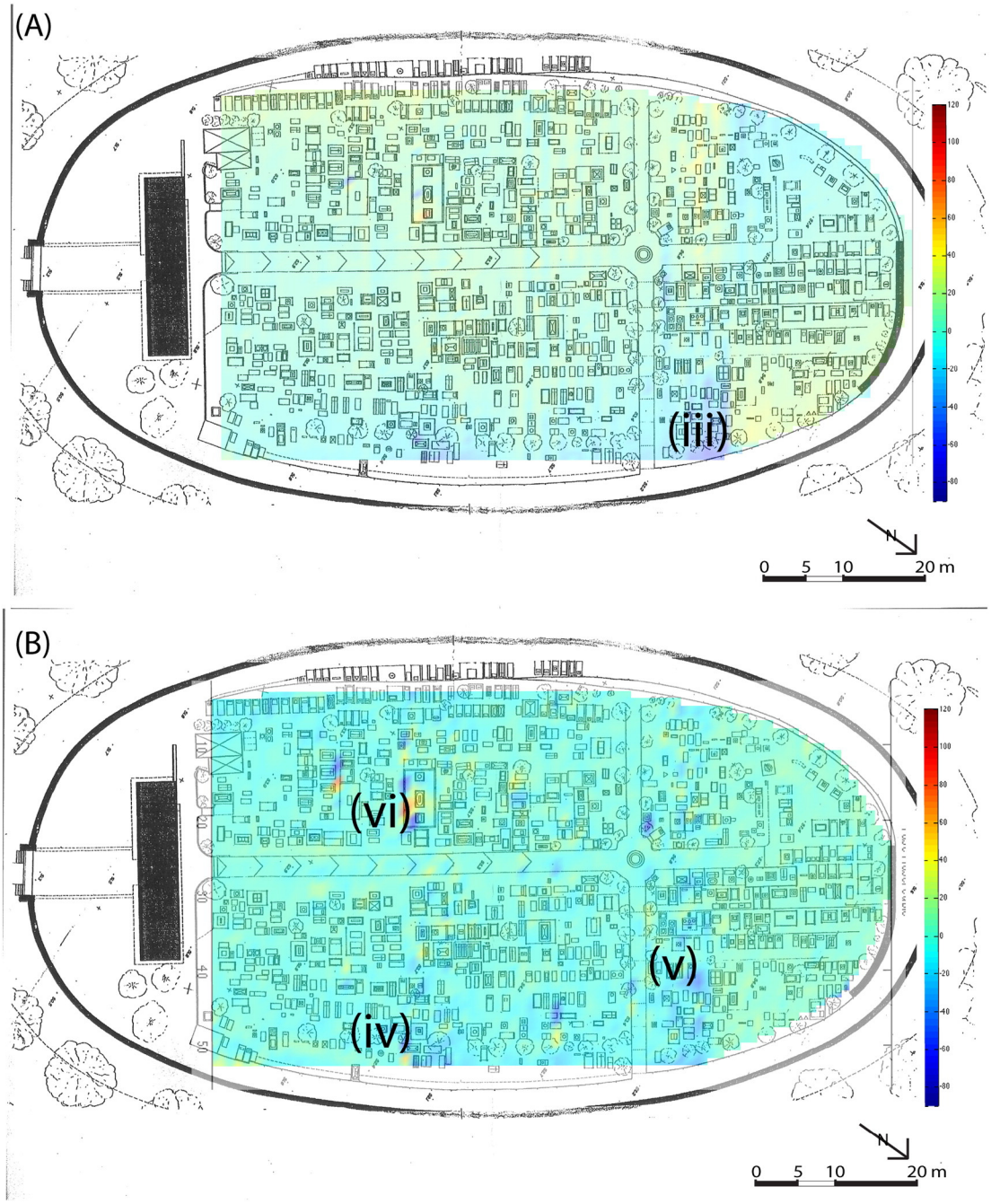

Fig. 9. 2D maps of the in-phase (A) and Karous-Hjelt filtered in-phase (B) component of the VLF-EM survey. (iv), (v), and (vi): areas with negative VLF-EM anomalies (cold colours) associated with lower conductive areas; (vi): positive VLF-EM anomalies (hot colours) more concentrated and associated with higher conductive areas.

All VLF profiles were processed to generate 2D maps of the in-phase and filtered in-phase components (Fig. 9A–B, respectively). In the in-phase map (Fig. 9A), a row-effect affecting the contour is more evident (Sundararajan et al., 2006). The zero contour lines (green areas in Fig. 9) in a Fraser filtered component map separate the conductive anomalies (positive values) from the resistive ones (negative values; Abbas et al., 2012). The lower values of the Karous-Hjelt filtered data indicate the higher value of resistivity (Bayrak and Şenel, 2012). The better results are obtained from the Karous-Hjelt filter, as the anomalies are more concentrated and detailed. The Karous-Hjelt filtered 2D map (Fig. 9B) shows areas with lower values ((iv) and (v) in Fig. 9B) and anomalies more concentrated ((vi) in Fig. 9B). Moreover, all the VLF profiles filtered by the Karous-Hjelt filter were processed to generate pseudo-sections of the current density. The Karous-Hjelt filter, in fact, has shown to be a quite good indicator of the depth of the current anomalies and can be used to assess their spatial distribution (Sundararajan et al., 2006; Khalil et al., 2010).

Among all the VLF pseudo-sections in Fig. 10, we show eight profiles (from 23 to 27 and from 55 to 57) orthogonal to the AA′ ERT (red line in the top plan) and coinciding with the resistive anomalies detected. Three parallel profiles to the ERT itself (T1-T3 in Fig. 10) were extracted and processed as a VLF line. The results show that a good correspondence between the conductive anomalies (hot colours at about 20 and 55 m in T1–T3 VLF profiles and blue colours from 10 to 25 m and from

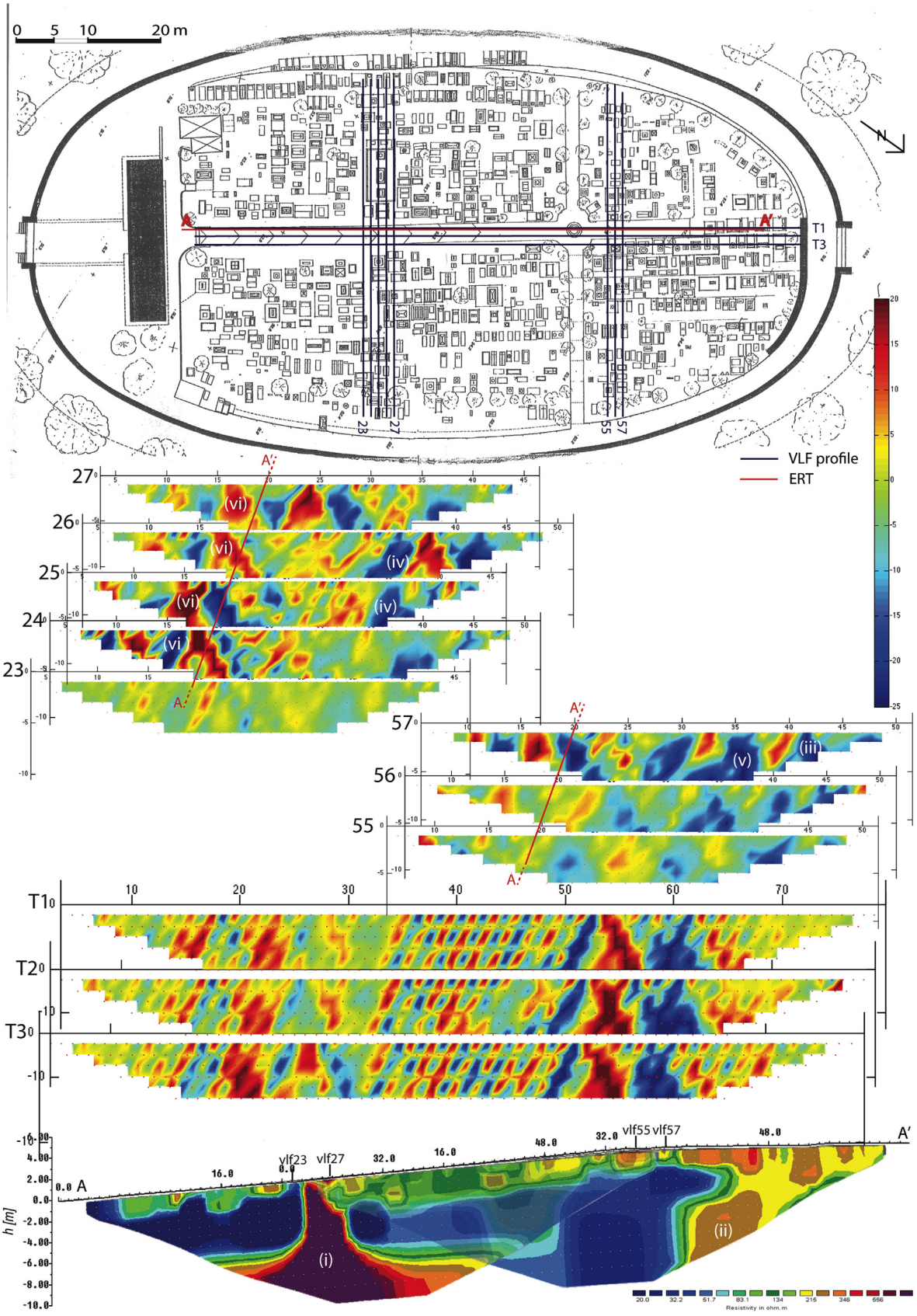

Fig. 10. Eight pseudo-sections (23–27 and 55–57) of current density from selected VLF-EM profiles orthogonal to the AA′ ERT (red line in the upper map and reported as resistivity section in the lower part of the figure) and filtered by the Karous-Hjelt and three parallel profiles to the ERT itself (T1–T3) extracted and processed as a VLF line. (i), (ii), (iii), (iv), and (v) are the same anomalies shown in Figs. 7 and 8. (For interpretation of the references to colour in this figure legend, the reader is referred to the web version of this article.)

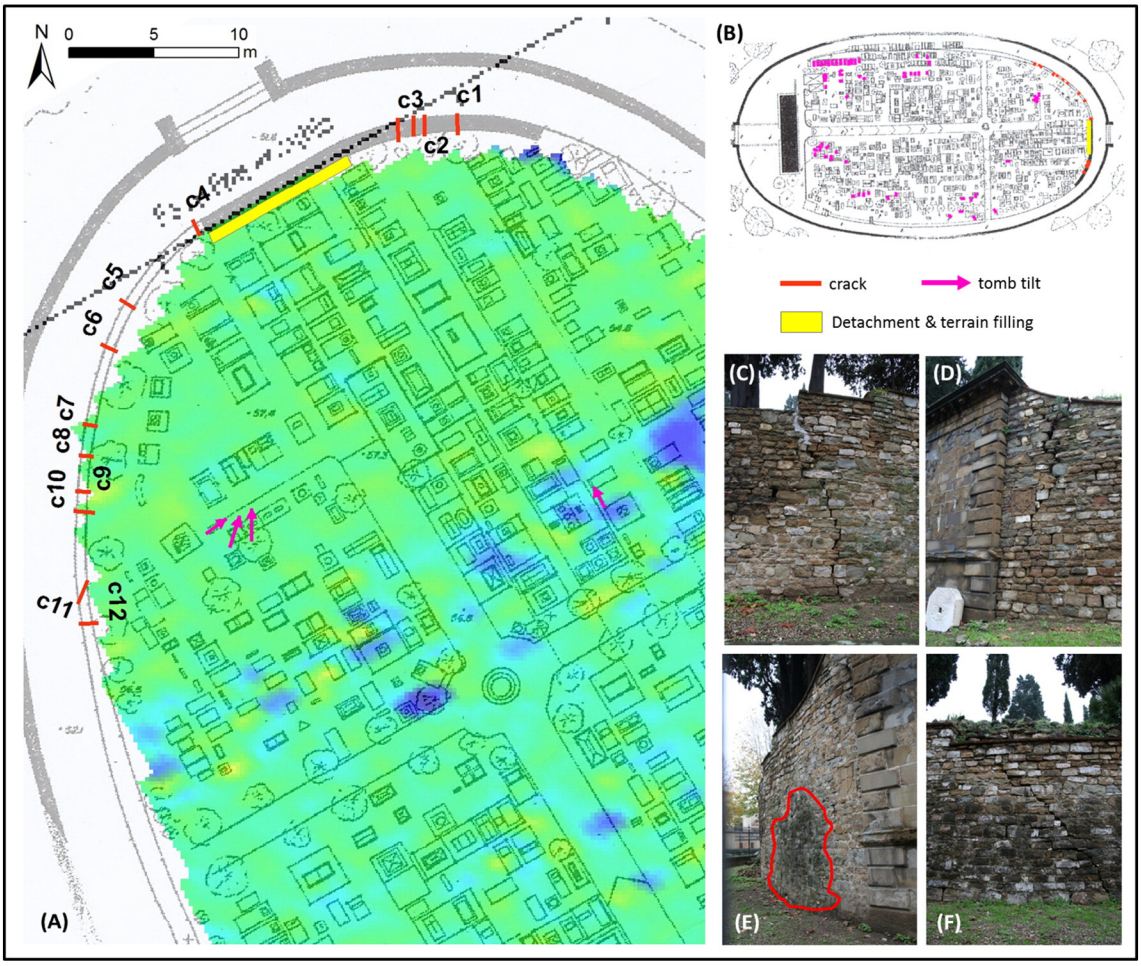

Fig. 11. (A) Crack pattern map onto the Karous-Hjelt filtered in-phase component of the VLF-EM survey of the northern sector of the English Cemetery, where fractures mainly concentrate compared with the (B) distribution of the observed tomb tilts. Detailed views of cracks (C) c3 and (D) c4 close to the monumental niche; (E) wet area (red line) over the exterior surface of the wall close to crack c3. (F) Crack c11 diagonally runs along the western wall (photo credit D. Tapete). (For interpretation of the references to colour in this figure legend, the reader is referred to the web version of this article.)

48 to 60 m in the AA′ ERT) and the resistive ones (cold colours at about 25 and 60 m in T1–T3 VLF profiles and anomalies (i) and (ii), respectively, in the AA′ ERT).

The greater positive and negative anomalies coincide with the tombs where surface movements were detected (i.e., anomaly (iii) in Figs. 9A and 10). Nevertheless, there is not a direct correspondence between the anomalies and the surface movements even though the resistive anomalies detected by the VLF-EM survey could be associated with subsuperficial voids or soil deformations. We cannot exclude that the surface movements, the impact of which are observed across the cemetery, took place earlier. In such a case, the recorded VLF anomalies might not have any correlation with the causes of the movements. The VLF time-lapse monitoring might provide further evidence to verify this hypothesis.

4.2. Surface damage assessment

The crack pattern survey highlights that fractures mostly run from top to bottom of the perimeter wall of the mound and concentrate in the northern part of the cemetery (Fig. 11A–B). This is the area of the retaining wall and the monumental stone façade dating back to Poggi's interventions in 1870 (Fig. 1C). This section coincides with the highest portion of the wall (about 7 m equalling the maximum elevation difference between the mound and the road level; cf. Section 2.1), where the terrain pressure is reasonably expected to be the highest owing to the full potential of the mound. Most of the cracks (c4 to c12) are distributed over the northwestern section of the wall facing the city centre (Fig. 11A); while a smaller group (c1 to c3) affects the other side, east of the central niche. The cracks closest to the niche are up to 5–7 cm wide and seem to isolate this portion of the wall (Fig. 11C–D). Therefore, this is the area classified at the highest risk of structural instability. This assessment is also based on the evidence that large areas of the exterior surface of the wall are persistently wet and covered by mosses (Fig. 11E). This is typically a sign that water from the rear ground is retained and not discharged and, therefore, can generate pressure against the stone wall. In addition, masonry detachment of up to 2 cm was observed at the top, behind the cornice of the monumental façade. In situ inspections confirmed that the mound terrain filled the cavity behind the stone façade and the central niche.

Cracks c7 to c10 identify another warning area, with crack c11 being located a few meters south (Fig. 11a). This runs diagonally with a NE-SW orientation and averages 5 cm wide, with gaps between the stone blocks up to 9.4 cm (Fig. 11F). The appearance of this crack suggests that ground motions are likely occurring along the natural topographic gradient of the mound. Although no signs of instability were observed over the overlying tombs, repair of the wall and consolidation works should be undertaken.

During the systematic field-walk survey no fractures were observed over the ground that could be associated with slope failure or ongoing collapses. Nevertheless, clusters of tombs were found tilted beyond the expected inclination that typically occurs in time caused by organic material deterioration and consequent terrain compaction (Fig. 12B).

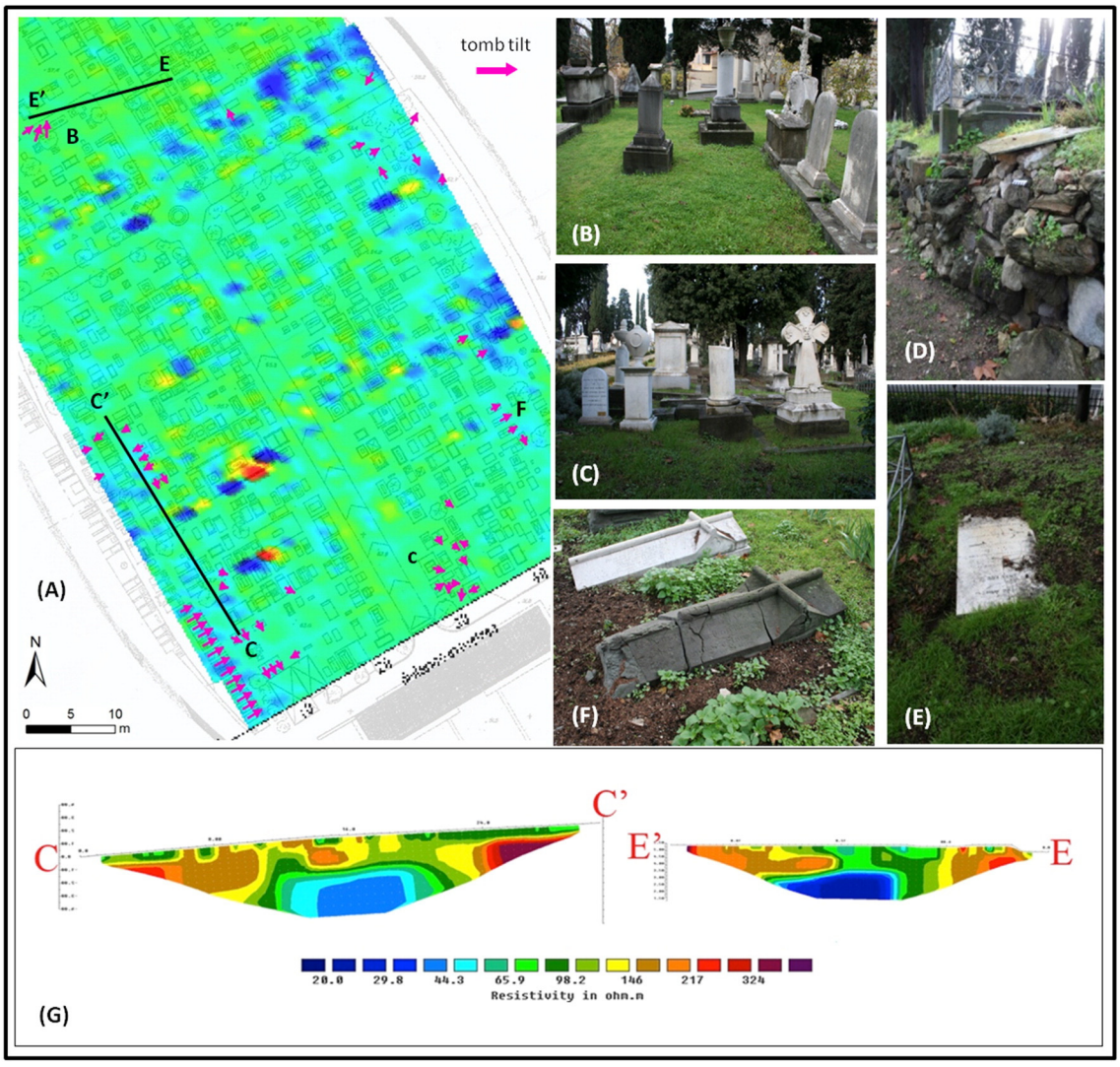

Fig. 12. (A) Tilt pattern map of the English Cemetery onto the Karous-Hjelt filtered in-phase component of the VLF-EM survey. In situ inspections revealed (B–C) clusters of tilted tombs concentrated in local sectors of the cemetery; (D–E) gravestones displaced along the slope and (F) damaged at an extent that the sarcophagi are severely broken (for location see lettering in picture (A)); (G) CC′ and EE′ ERTs (photo credit D. Tapete).

Fig. 12A shows the spatial distribution of patterns of tomb tilt, which suggests an adaptation of the tombs to local shallow phenomena of soil compaction and collapse. This is, for instance, the case of the cluster of tilted tombs in the northwestern quarter of the cemetery (Fig. 12B) and those at the eastern corner of the central pathway (Fig. 12C). Interestingly most of the clusters are distributed in the southern quarters of the mound (Fig. 12A) where this type of evidence might not have been expected given the low value of the slope angle. On the other side, some gravestones located close to the mound edge have been displaced along the slope direction (Fig. 12D–E). Damage can be quite severe with marble slabs and stone sarcophagi partially or fully broken (Fig. 12F).

The CC′ and EE′ ERTs (Fig. 12G), which were acquired near the tomb clusters in the northwestern and southwestern sectors (Fig. 12A–B), highlight a correspondence between the tilted tombs on the surface and the resistive area at about 1–3 m depth. Furthermore, the filtered VLF-EM map (Fig. 12A) shows negative values (associated with more resistive values) in these areas. These resistive values might indicate the presence of coarser material subject to compaction phenomena.

Although, as explained in Section 4.1, some possible correlation was found between the tilt patterns and the resistivity anomalies, the field evidence proves that the tombs were impacted at some extent by local processes of soil compaction and ground instability. This outcome of the survey should be accounted for as part of the plans for maintenance and restoration of the cemetery. Notably the combination of VLF-EM and 2D-ERT could also be very useful to detect subsoil anomalies related to areas of water accumulation that can cause superficial subsidence, especially if these techniques are implemented according to a schedule of regular acquisitions across various seasons.

5. Conclusions

The geophysical approach presented in this paper allows subsurface and surface data to be collected and integrated to assess holistically the nature and current condition of mounds that represent topographic anomalies in flat urban landscapes. With no need of expensive, time-consuming, and invasive ground investigations, this approach offers an improved geognostic knowledge in urban environments to inform the design of maintenance and restoration measures, especially when the mounds have historic and cultural value and are used for civilian purposes.

The experiment undertaken in the English Cemetery of Florence is a proof-of-concept of the opportunities that this method can offer for implementation in urban contexts. In agreement with the historical archival records, our investigations prove that the Florentine mound has been hugely modified from the former natural setting, thus becoming a remarkable anthropogenic feature at the boundary of the city centre.

The VLF-EM tomographies reveal the presence of resistive anomalies with values >300 and 400 Ωm. Given the location and the shape of the geophysical signals, these anomalies might refer to the perimeter wall that was attached to the medieval city walls prior to their demolition undertaken in the 1870s.

Factors increasing the exposure of the cemetery to groundwater-related instability and local collapses include the mixed natural and artificial character of the mound, the varied morphology and topography, the tree coverage, and the high density of tombs. While ERTs and VLF-EM sections do not present evidence of an apparent correlation with the causes of tomb and ground movements, the maps of tilt and crack patterns clearly indicate where local-scale processes of soil compaction and ground instability are manifesting and should be remediated to prevent failure.

Acknowledgements

The geophysical prospection in the English Cemetery of Florence was carried out in the framework of the cooperation between the Departments of Engineering and of History, Archaeology, Geography, Fine & Performing Arts, University of Florence. D. Tapete contributed to the fieldwork, data integration and interpretation and provided the conceptual framework within the urban geoscience research remit. The authors thank Chiesa Evangelica Riformata Svizzera and Julia Bolton Holloway for their precious collaboration and availability. The authors are also grateful to Sebastian Uhlemann for the helpful comments on an earlier version of this manuscript, and to the three anonymous reviewers and the Editor Dr. R.A. Marston for their help improving the manuscript. D. Tapete publishes with the permission of the Executive Director of the British Geological Survey (NERC).

References

Abbas, A.M., Khalil, M.A., Massoud, U., Santos, F.M., Mesbah, H.A., Lethy, A., Soliman, M., Ragab, E.-S.A., 2012. The implementation of multi-task geophysical survey to locate Cleopatra tomb at tap-Osiris Magna, Borg El-Arab, Alexandria, gypt "phase II". NRIAG-JAG 1, 1–11.
Ahnert, F., 1998. Introduction to Geomorphology. Arnold, London.
Andrews, D., Bedford, J., Bryan, P., 2015. Metric Survey Specifications for Cultural Heritage. Historic England Publications 978-1-84802-296-6, p. 240.
Barone, P.M., Swanger, K.J., Stanley-Price, N., Thursfield, A., 2016. Finding graves in a cemetery: preliminary forensic GPR investigations in the non-Catholic cemetery in Rome (Italy). Measurement 80, 53–57.
Bathrellos, G.D., 2007. An overview in urban geology and urban geomorphology. Bull. GSG 40, 1354–1364.
Bayrak, M., Şenel, L., 2012. Two-dimensional resistivity imaging in the Kestelek boronarea by VLF and DC resistivity methods. J. Appl. Geophys 82, 1–10.
Chengtai, D., 1996. An approach to theory and methods of urban geomorphology. Chin. Geogr. Sci 6 (1), 88–95.
Coates, D., 1976. Urban geomorphology, Colorado, USA. Geol. Soc. Am. Spec. Pap 174, 166.
Comune di Firenze, 2015a. Comune di Firenze - Sistema Informativo Geologico del Sottosuolo. http://maps.comune.fi.it/geo/.
Comune di Firenze, 2015b. Comune di Firenze. Piano Regolatore Generale. http://prg.comune.fi.it.
Cooke, R.U., 1976. Urban geomorphology. Geogr. J 142 (1), 59–65.
Dahlin, T., 2001. The development of DC resistivity imaging techniques. Comput. Geosci 27, 1019–1029.
Douglas, I., 2010. Urban geomorphology. The Routledge Handbook of Urban Ecology http://dx.doi.org/10.4324/9780203839263.ch14.
Drahor, M.G., 2011. A review of integrated geophysical investigations from archaeological and cultural sites under encroaching urbanization in İzmir, Turkey. Phys. Chem. Earth 36, 1249–1309.
Ford, J., Kessler, H., Cooper, A.H., Price, S.J., Humpage, A.J., 2010. An enhanced classification for artificial ground. British Geological Survey Open Report, OR/10/036, p. 32.
Fraser, D.C., 1969. Contouring of VLF-EM data. Geophysics 34, 958–967.
Gaffney, C., 2008. Detecting trends in the prediction of the buried past: a review of geophysical techniques in archaeology. Archaeometry 50 (2), 313–336.
Goodman, D., Piro, S., 2013. GPR remote sensing in archaeology. Geotechnologies and the Environment Vol. 9. Springer-Verlag, Berlin Heidelberg.
Griffiths, D.H., Barker, R.D., 1994. Electrical imaging in archaeology. J. Archaeol. Sci 21 (2), 153–158.
Hudson, P., Goudie, A., Asrat, A., 2015. Human impacts on landscapes sustainability and the role of geomorphology. Z. Geomorphol. Suppl 59 (2), 1–5.
Karous, M., Hjelt, S.E., 1983. Linear filtering of VLF dip-angle measurements. Geophys. Prospect 31, 782–794.
Khalil, M.A., Abbas, A.M., Santos, F.A.M., Mesbah, H.S.A., Massoud, U., 2010. VLF-EM study for archaeological investigation of the labyrinth mortuary temple complex at Hawara area, Egypt. Near Surf. Geophys 8, 203–212.
Koefoed, O., 1979. Geosounding Principles 1: Resistivity Sounding Measurements. Elsevier Science Publishing Company, Amsterdam.
Leckebusch, J., 2000. Two-and-three-dimensional ground-penetrating radar surveys across a medieval choir: a case study in archaeology. Archaeol. Prospect 7, 189–200.
Loke, M.H., 2012. Tutorial: 2-D and 3-D Electrical Imaging Surveys. Geotomo Software, Malaysia.
Loke, M.H., Barker, R.D., 1996a. Rapid last-squares inversion of apparent resistivity pseudosections using a quasi-Newton method. Geophys. Prospect 44 (1), 131–152.
Loke, M.H., Barker, R.D., 1996b. Practical techniques for 3D resistivity surveys and data inversion. Geophys. Prospect 44 (3), 499–523.
Loke, M.H., Acworth, I., Dahlin, T., 2003. A comparison of smooth and blocky inversion methods in 2D electrical imaging surveys. Explor. Geophys 34 (3), 182–187.
Loke, M.H., Wilkinson, P.B., Chambers, J.E., 2010a. Fast computation of optimized electrode arrays for 2D resistivity surveys. Comput. Geosci 36 (11), 1414–1426.
Loke, M.H., Wilkinson, P.B., Chambers, J.E., 2010b. Parallel computation of optimized arrays for 2-D electrical imaging surveys. Geophys. J. Int. 183 (3), 1302–1315.
Loke, M.H., Chambers, J.E., Rucker, D.F., Kuras, O., Wilkinson, P.B., 2013. Recent developments in the direct-current geoelectrical imaging method. J. Appl. Geophys 95, 135–156.
McMillan, A.A., Powell, J.H., 1999. BGS rock classification scheme volume 4. Classification of artificial (man-made) ground and natural superficial deposits - applications to geological maps and datasets in the UK. British Geological Survey Research Report, RR 99–04, p. 66.
METS, 2015. Piano straordinario di telerilevamento. http://www.pcn.minambiente.it/GN/progetti/piano-straordinario-di-telerilevamento.
Price, S., Ford, J., Kessler, H., Cooper, A., Humpage, A., 2004. Artificial ground. Mapping our impact on the surface of the earth. Earthwise 20, 30–31.
Reynolds, J.M., 2011. An Introduction to Applied and Environmental Geophysics. second ed. John Wiley & Sons, England.
Smith, B.D., Ward, S.H., 1974. On the computation of polarization ellipse parameters. Geophysics 39, 867.
Sundararajan, N., Babu, V.R., Prasad, N.S., Srinivas, Y., 2006. VLFPROS – a Marlab code for processing of VLF-EM data. Comput. Geosci 32, 1806–1813.
Tapete, D., Cigna, F., 2012. Rapid mapping and deformation analysis over cultural heritage and rural sites based on persistent scatterer interferometry. Int. J. Geophys 19 http://dx.doi.org/10.1155/2012/618609.
Tapete, D., Morelli, S., Fanti, R., Casagli, N., 2015. Localising deformation along the elevation of linear structures: an experiment with space-borne InSAR and RTK GPS on the Roman aqueducts in Rome, Italy. Appl. Geogr 58, 65–83.
Thornbush, M., 2015. Geography, urban geomorphology and sustainability. Area 47, 350–353.
Tuscany Region, 1994. Pericolosità idraulica media secondo il D.C.r. 230 Delibera del Consiglio della Regione Toscana 21 giugno 1994, n.230. http://www.architoscana.org/Normativa/ns_reg_toscana/tos_90-95/DEL.C.R.230-94.html.
Vitek, J.D., 2013. Geomorphology: perspectives on observation, history, and the field tradition. Geomorphology 200, 20–33.